C. R. Chimie 21 (2018) 104–111

Contents lists available at ScienceDirect

Comptes Rendus Chimie

www.sciencedirect.com

Full paper/Mémoire

Novel PEI–AuNPs–Mn^{III}PPIX nanocomposite with enhanced peroxidase-like catalytic activity in aqueous media

Huifang Xie**, Shumei Gu, Jingyi Zhang, Qiong Hu, Xuehua Yu, Jinming Kong*

School of Environmental and Biological Engineering, Nanjing University of Science and Technology, Nanjing 210094, PR China

ARTICLE INFO

Article history:
Received 4 September 2017
Accepted 30 November 2017
Available online 17 January 2018

Keywords:
Peroxidase-like activity
Mn porphyrin
Gold nanoparticles
Polyethyleneimine
Activation of H_2O_2

ABSTRACT

Mn porphyrin provides a possibility to constitute the novel mimic catalyst with peroxidase-like activity. A simple method for preparing a novel catalyst PEI–AuNPs–Mn^{III}PPIX, used in aqueous media, was presented in this paper. The covalent anchoring of Mn^{III}PPIX and PEI were verified, meanwhile gold nanoparticles with the diameter less than 10 nm were dispersed uniformly and stably. The remarkable peroxidase-like catalytic activity of PEI–AuNPs–Mn^{III}PPIX was displayed in the oxidative degradation of azo dye acid orange 7 (AO7) as the model reaction in the presence of trace of H_2O_2. The synergistic effects of PEI–AuNPs and Mn^{III}PPIX on the enhancement of catalytic activity were observed at pH 2.0. Possible pathways involving in the formation of active radicals are proposed. The construction of PEI–AuNPs–Mn^{III}PPIX nanocomposite offers a new insight into the application of Mn porphyrin upon activation of H_2O_2, which have potential applications in many fields.

1. Introduction

Synthetic metalloporphyrins are regarded as an ideal platform for catalysis with peroxidase-like activity and draw much interest because of their versatile applications such as epoxidation of alkenes, oxidative degradation of xenobiotics, biosensors, and so on [1–6]. Among the biomimetic metalloporphyrins, iron (Fe) and manganese (Mn) stick out, due to their availability and importance of redox cofactors. In sharp contrast to Fe, analogous Mn porphyrin–catalyzed oxidations remained undeveloped. Mn reconstituting heme proteins such as horseradish peroxidase (Mn^{III} HRP) [7], microperoxidase-8 (Mn^{III}MP-8) [8], cytochrome *c* peroxidase (Mn^{III}C*c*P) [9], and myoglobin (Mn^{III}Mb) [10] have been prepared, but showed much lower reactivity toward hydrogen peroxide (H_2O_2).

Efforts were made to improve their activities by introducing amino acid residues with imidazole functional groups [11–13]. Similar works have been done for synthetic Mn porphyrins. The additives containing nitrogen such as imidazole and its derivatives [6,14,15] and pyridine derivatives [16] are most applied because of the axial ligand effect due to the formation of hydrogen bond between nitrogen and H_2O_2 coordinated at the Mn center. This effect is generally more pronounced in the reactions catalyzed by Mn^{III} porphyrins [17]. Other methods reported with higher catalytic activation of H_2O_2 include the choice of Mn porphyrin nanocomposite with the tail of carboxylic groups [6,14], the addition of a carboxylic acid [16], and the immobilization of Mn porphyrin to supports (amino-functionalized montmorillonite [17], chlorinated graphene oxide [18], modified multiwall carbon nanotube [19], and so on).

Because most synthetic models are designed to function in generally organic homogeneous solution rather than the environmentally benign aqueous media [5], water-soluble mimics come into notice. The

* Corresponding author.
** Corresponding author.
E-mail addresses: huifangxie@hotmail.com (H. Xie), j.kong@njust.edu.cn (J. Kong).

https://doi.org/10.1016/j.crci.2017.11.010
1631-0748/

biocompatible polymer with imidazole groups and carboxymethylated imidazolium groups was used to support Mn porphyrin in the preparation of the water-soluble mimics [20].

Murakami and Konishi [21] found the remarkable cocatalytic effect of gold nanoclusters on olefin oxidation catalyzed by the Mn porphyrin nanocomposite. Au nanoparticles (AuNPs) have enormous applications due to their unique physicochemical features such as biocompatibility, amphilicity, larger surface carrier capabilities, and gold electronic conductivity [22–24]. However, their tendency of agglomeration needs to be prevented for effective use. To synthesize well-dispersed AuNPs, various nanoreactor systems have been used; among them, polyethyleneimine (PEI) displays the reduction of $AuCl_4^-$ to AuNPs under mild conditions and steric stabilization for AuNPs [25–28]. In our previous study, PEI–AuNPs–hemin nanocomposite was proved to have a much-improved peroxidase-like catalysis for decomposing H_2O_2 [28], which indicated that the PEI–AuNPs can enhance the catalytic activity of metalloporphyrins.

In this study, we designed and synthesized a nanocomposite of Mn^{III} protoporphyrin IX chloride (Mn^{III}PPIX) associated with PEI–AuNPs, which is in a stable colloidal state in water. The oxidative degradation of azo dyes is often used to test the efficiency of peroxidase and its mimic system [29–36]. We herein used PEI–AuNP–Mn^{III}PPIX nanocomposite-catalyzed oxidative degradation of acid orange 7 (AO7), a kind of azo dye, as the model reaction and reported the notable peroxidase-like catalytic ability of this nanocomposite. The possible mechanisms are also proposed.

2. Experimental section

2.1. Materials and apparatus

All the reagents used here were of analytical grade. In particular, branched PEI (average molecular weight, M_w = 25 kDa) was purchased from J&K Scientific Ltd. (Shanghai, China). Hydrogen tetrachloroaurate(III) tetrahydrate ($HAuCl_4 \cdot 4H_2O$) was purchased from Sigma–Aldrich (St. Louis, MO) and Mn^{III}PPIX from Frontier Scientific Inc. AO7 (C.I. 15510) was purchased from Beijing Chemical Reagents Co.

UV–vis spectra were recorded using a UV-3600 UV–VIS–NIR spectrophotometer (Shimadzu, Japan). Fourier transform infrared (FTIR) spectrum analysis was performed using an FTIR-8400S spectrophotometer (Shimadzu, Japan). Transmission electron microscopy (TEM) image was obtained using a JEOL JEM-2100 transmission electron microscope at an acceleration voltage of 200 kV.

2.2. Preparation and characterization of PEI–AuNPs–Mn^{III}PPIX

PEI–AuNPs were synthesized as described in our previous report [28]. Then, the PEI–AuNPs were added into a 0.1 mM Mn^{III}PPIX solution (in 0.1 M phosphate-buffered saline [pH 9.0]) in a stoichiometric ratio of 1:0.12. The mixture was stirred at 25°C. After 1 h, the mixture was centrifuged at 14,000 rpm for 60 min, and then the precipitate was washed and centrifuged again in ultrapure water for three times. So prepared PEI-AuNPs-Mn^{III}PPIX was dispersed in water with a final concentration of 0.5 mg/mL and stored at 4°C in the dark for further use.

2.3. Catalytic experiments of PEI–AuNPs–Mn^{III}PPIX

AO7 stocking solution (1000 mg/L) was prepared by dissolving it in 0.1 M phosphate-buffered saline at various pHs between 1.0 and 9.0. The AO7 oxidative degradation was carried out at 25°C in the dark for 120 min as follows: certain amounts of the catalyst were added into the 24 mg/L AO7 solution and the reaction was initiated by adding precalculated amount of H_2O_2. The residual AO7 was quantified by spectrophotometric assay at 484 nm, the maximum peak of AO7. Control reactions in different systems were carried out.

3. Results and discussion

3.1. Preparation and characterization of the catalyst, PEI–AuNPs–Mn^{III}PPIX

Scheme 1 shows the preparation route for PEI–AuNPs–Mn^{III}PPIX. PEI was used as a reducing and protective agent to prepare the PEI–AuNPs by one-step thermal process synthesis [28]. Next, PEI–AuNPs–Mn^{III}PPIX was prepared by an amidation reaction between carboxyl groups of porphyrin and the amino groups of PEI–AuNPs. Thus, Mn^{III}PPIX is heterogenized and protected from forming dimer, which was supposed to be one of the most important deactivation reasons for metal porphyrin [18].

The prepared catalyst was in a stable colloidal state in water and was characterized using UV–vis spectroscopy and FTIR (Fig. 1).

The UV–vis spectrum of Mn^{III}PPIX shows three absorption peaks at 370, 464, and 554 nm, respectively. Compared to the spectra of PEI–AuNPs and Mn^{III}PPIX, all three peaks were red shifted, which suggests that the conjugation is formed in the PEI–AuNPs–Mn^{III}PPIX nanocomposite [37,38]. The calculated diameter of AuNPs was 9.6 nm according to Haiss's theory [39]. The FTIR spectrum of the PEI–AuNPs–Mn^{III}PPIX features several characteristic bands. The strong and broad band near 3450 cm^{-1} belongs to stretching vibration of NH from PEI. There are absorption peaks of stretching vibration of NH_2^+ at 2948, 2843, and 2300 cm^{-1}. The peak at 1632 cm^{-1} can mainly be assigned to a C=O stretching in carboxyl or amide groups. The peaks at 1469 and 1017 cm^{-1} are attributed to the NH deformation vibration and CN stretching vibration. The informative spectroscopic data confirmed the covalent anchoring of Mn^{III}PPIX and PEI.

The morphology of PEI–AuNPs–Mn^{III}PPIX was further characterized by TEM, and Fig. 2 presents its representative TEM image and the size distribution.

As shown in Fig. 2, the PEI–AuNPs–Mn^{III}PPIX had an approximately spherical morphology and dispersed uniformly with the average diameter of 9.4 nm (200 particles

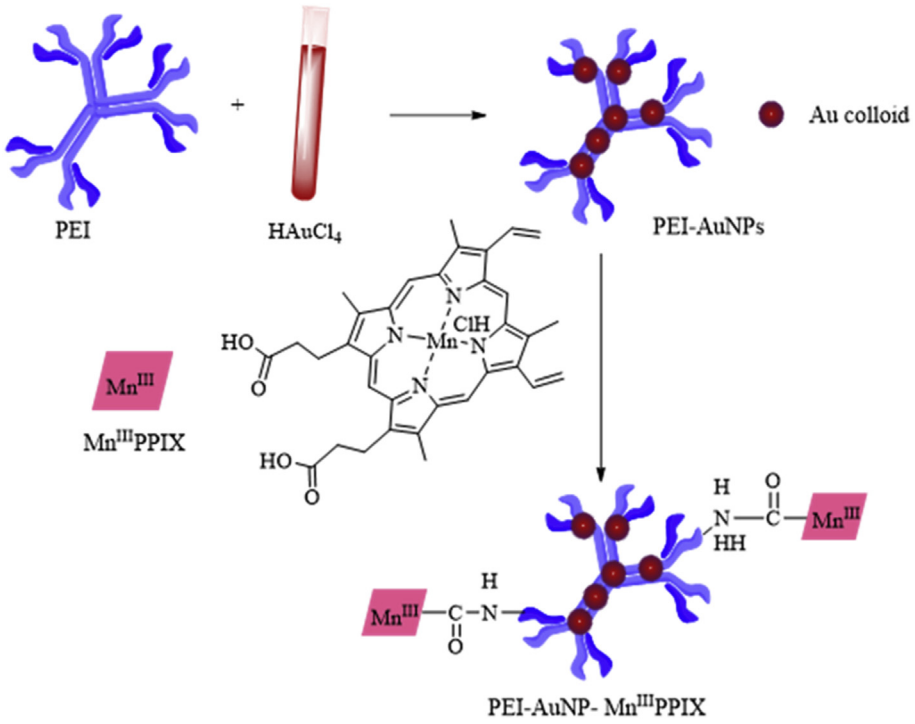

Scheme 1. Preparation route of the PEI–AuNPs–Mn^{III}PPIX nanocomposite.

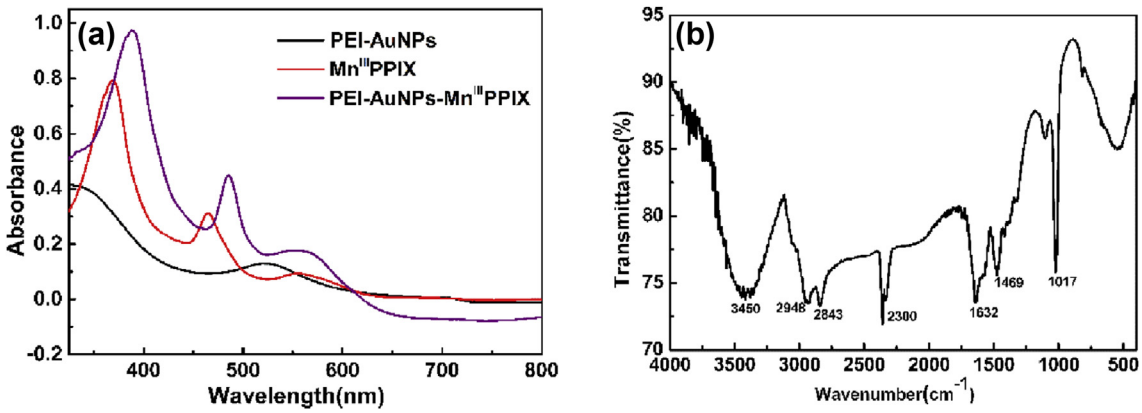

Fig. 1. (a) UV–vis absorption spectra of PEI–AuNPs, Mn^{III}PPIX, and PEI–AuNPs–Mn^{III}PPIX nanocomposites; (b) FTIR spectrum of the PEI–AuNPs–Mn^{III}PPIX nanocomposite.

counted), and this matched well with the calculated results mentioned previously.

3.2. Peroxidase-like activities

To examine the catalytic activity of as-prepared PEI–AuNPs–Mn^{III}PPIX, we chose AO7, a typical azo dye as a probe of organic pollutants, which can be degraded by native peroxidase [40,41]. Fig. 3 shows the spectral changes of AO7 in different systems.

No obvious change of AO7 spectra is observed when Mn^{III}PPIX is present. The presence of PEI–AuNPs and PEI–AuNPs–Mn^{III}PPIX induced a decrease in the absorbance at 485 nm, which could be due to the adsorption of AO7 on the nanocomposite. It is interesting that there was an obvious decrease when PEI–AuNPs–Mn^{III}PPIX was added, indicating that the combination of Mn^{III}PPIX and PEI–AuNPs played a crucial role. The presence of H_2O_2 enhanced the AO7 degradation catalyzed by Mn^{III}PPIX and PEI–AuNPs–Mn^{III}PPIX and the most thorough degradation of AO7 achieved in the PEI–AuNPs–Mn^{III}PPIX/H_2O_2 system. The results prove the remarkable activity of the novel PEI–AuNPs–Mn^{III}PPIX nanocomposite on the activation of H_2O_2.

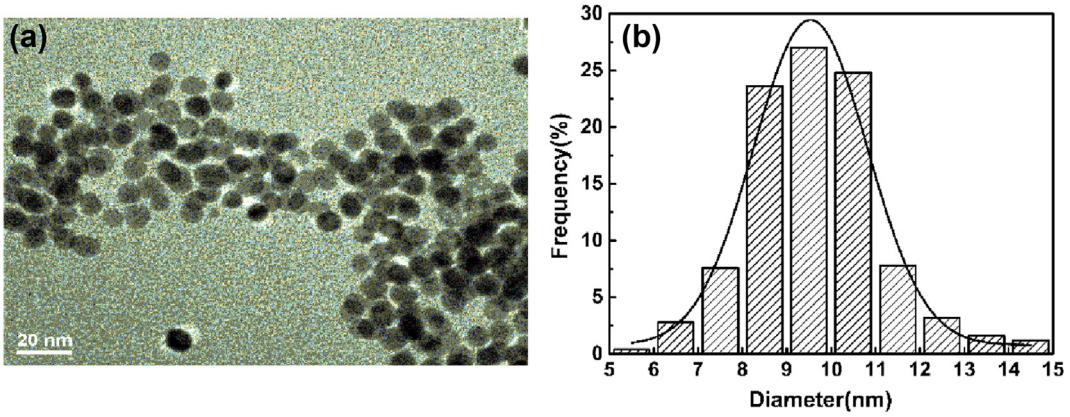

Fig. 2. (a) TEM image of the PEI–AuNPs–Mn^{III}PPIX nanocomposite. (b) The size distribution histogram of the immobilized AuNPs.

3.3. Factors affecting the degradation of AO7 in the PEI–AuNPs–$Mn^{III}PPIX/H_2O_2$ system

3.3.1. Catalyst dosage

Fig. 4 presents the degradation profile at different catalyst dosages ranging from 0.8 to 4.0 mg/L. As shown in Fig. 4a, the profile of normalized concentrations with time follows an exponential pattern, which may describe the degradation of AO7 according to the pseudo-first-order kinetic reaction:

$$-\frac{dC_{AO7}}{dt} = k_{obs}C_{Ao7} \quad (1)$$

$$\ln\frac{C_{AO7}}{C_0} = -k_{obs}t \quad (2)$$

where C_{AO7} and C_0 represent the concentration of AO7 (mg/L) at time t and the initial time. k_{obs} is the pseudo-first-order rate constant (min^{-1}) for the degradation of AO7. k_{obs} were deduced from the linear fitting of $\ln(C/C_0)$ versus time.

The k_{obs} increased significantly as a function of the dosage from 0.8 to 2.4 mg/L (Fig. 4b). Such enhancement in degradation was ascribed to the increased number of active catalytic sites, which are responsible for the formation of active radicals. Further increase in dosage (>3.2 mg/L) does not increase the k_{obs} obviously, which may be limited by the rate-limiting step of the cleavage of the O–O or O–H bond in the intermediate where H_2O_2 is coordinated to the catalyst [4].

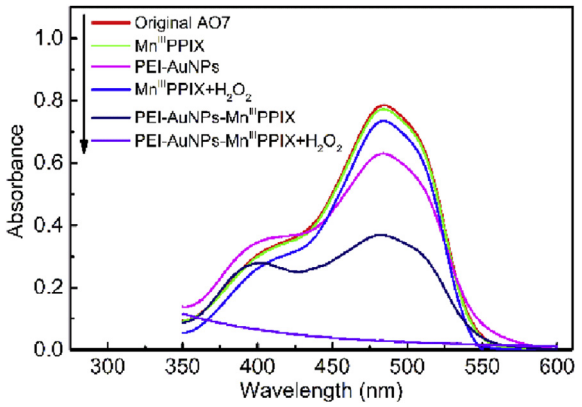

Fig. 3. UV–vis spectra of AO7 and its change in different systems.

3.3.2. pH value

pH is another important parameter in the peroxidase-like catalytic reaction. Fig. 5 shows the degradation profile of AO7 and k_{obs} between pH 1.0 and 9.0 and the maximum k_{obs} was achieved at pH 2.0. pH value affects the structure of azo dyes, and hydrozone is the main form in the acidic medium with more susceptibility to oxidation [42]. On the other hand, pH plays an important role in the transformation of H_2O_2 coordinated to the metal porphyrin, which is consequently converted to an active intermediate [12,43].

3.3.3. H_2O_2 concentration

Fig. 6 depicts the degradation profile of AO7 and k_{obs} at different H_2O_2 concentrations.

As the H_2O_2 concentration increased to 1.5 mM, nearly complete degradation of AO7 was achieved within 120 min. However, the degradation ratio and reaction rate decreased when the H_2O_2 concentration increased to 2.0 mM. Suppose AO7 is completely mineralized according to the reaction:

$$C_{16}H_{11}N_2O_4S^- + 42H_2O_2 \rightarrow 16CO_2 + 2NO_3^- + SO_4^{2-} + 3H^+ + 46H_2O$$

the amount of H_2O_2 needed is supposed at least 42-folds of the initial mole concentration of AO7. However, the consumed H_2O_2 in the PEI–AuNPs–Mn^{III}PPIX catalytic process was only 21.4-folds of the initial concentration of AO7, which means that more reactive oxidants play important roles in the degradation of AO7. In a kind of heterogeneous Fenton-like system (GO–Fe_3O_4 nanocomposite/H_2O_2), the initial 35 mg/L AO7 is reported to be oxidative degradation by 220-fold H_2O_2 [44]. In HRP/H_2O_2

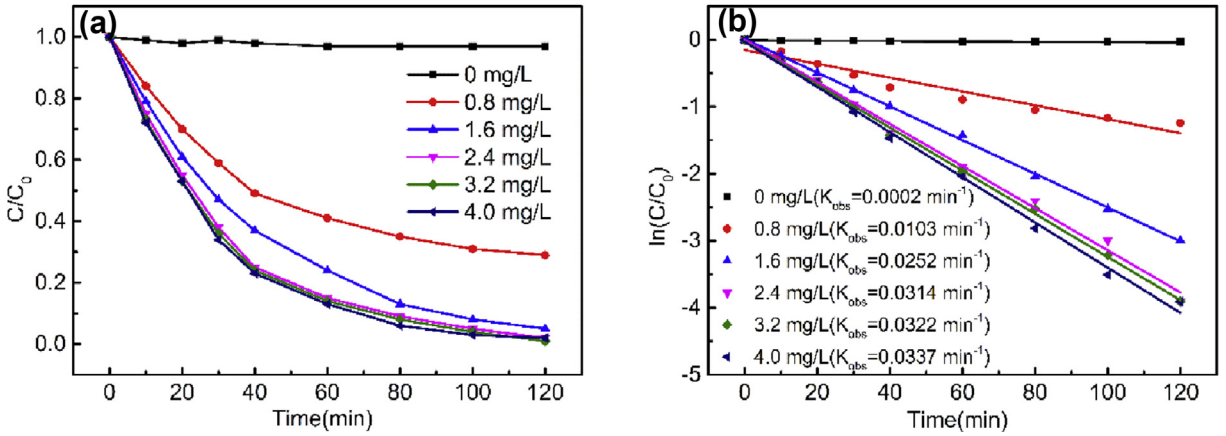

Fig. 4. (a) Effect of catalyst dosage on the degradation profile of AO7 and (b) the pseudo-first-order rate constant (AO 24 mg/L, pH 2.0, H_2O_2 1.5 mM).

system, the 11.32 mg/L AO7 is degraded by 25-fold H_2O_2 [40] and in a *Coprinus cinereus* peroxidase/H_2O_2 system, the 40 mg/L AO7 is degraded by 34-fold H_2O_2 [41]. So it can be inferred that PEI–AuNPs–Mn^{III}PPIX has high peroxidase-like catalytic activity for H_2O_2 to produce high active oxidant species.

3.4. Possible mechanism

In Mn porphyrin–catalyzed system, the homolysis of O–O in Mn peroxide with generation of •OH radicals [4,8,10,12,13,45] supposed as to the main pathway (see Scheme 2(A)). In the present study, *tert*-butyl alcohol (TBA) [46] and methyl alcohol (MeOH) [47] are selected as the scavengers. Fig. 7 proves the obvious role of •OH radicals during the degradation of AO7. The degradation ratios decreased from 97% to 33% and 45%, respectively, in the presence of TBA and MeOH and the k_{obs} decreased 10.2% and 15.0% correspondingly. The results show that degradation of AO7 associated with the generation of •OH radicals catalyzed by PEI–AuNPs–Mn^{III}PPIX is one important possible pathway. By comparing the inhibition effects of •OH scavengers on the degradation of azo dyes to that in typical •OH radicals' driving process [47], it is concluded that degradation of AO7 in the PEI–AuNPs–Mn^{III}PPIX/H_2O_2 system is not merely driven by •OH radicals.

The homolysis of O–O with generation of •OH radicals was thought to cause the lower reactivity of Mn porphyrin [13]. Many efforts have been made to enhance the activity of Mn^{III} porphyrin by adjusting the microenvironment of Mn^{III} in porphyrin [2,13,48–50]. Here, PEI–AuNPs are induced into the system to improve the catalytic activity. Concerning the catalytic system and the results of scavenging •OH radicals, we proposed the enhancing mechanisms of Mn^{III} porphyrin activity in the PEI–AuNPs–Mn^{III}PPIX/H_2O_2 system. The possible reaction pathways for the activation of H_2O_2 by PEI–AuNPs–Mn^{III}PPIX can be described as presented in Scheme 2 (B) and (C).

First, the presence of the carboxyl group in Mn^{III}PPIX affords a suitable tail for the coordination and activation of H_2O_2 due to the formation of an acyperoxy-Mn^{III} intermediate, in which the heterolytic cleavage of the O–O bond is favored by the good leaving of the carboxylate [6,14]. Thus,

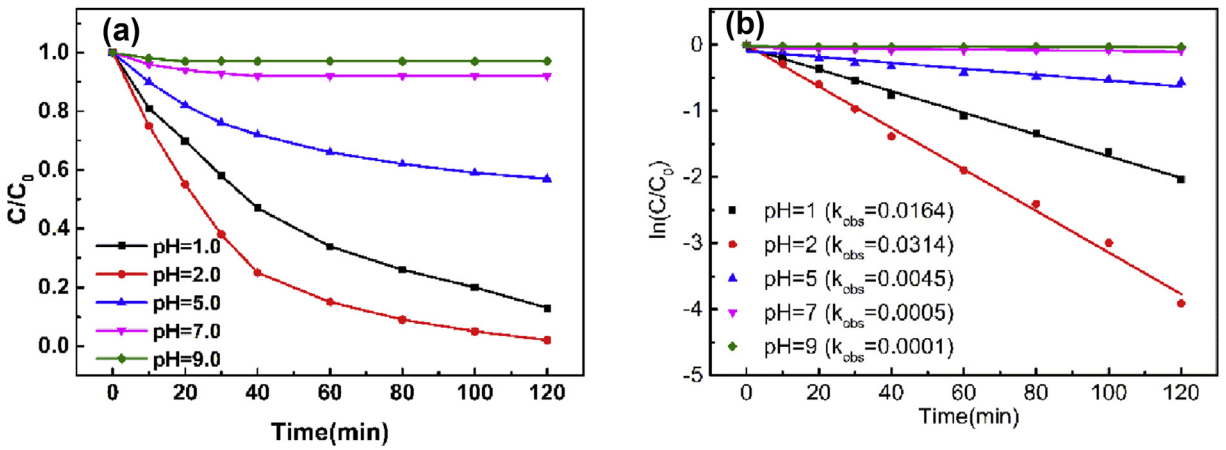

Fig. 5. (a) Effect of pH on the degradation profile of AO7 and (b) the pseudo-first-order reaction rate constant (AO 24 mg/L, PEI–AuNPs–Mn^{III}PPIX 2.4 mg/L, H_2O_2 1.5 mM).

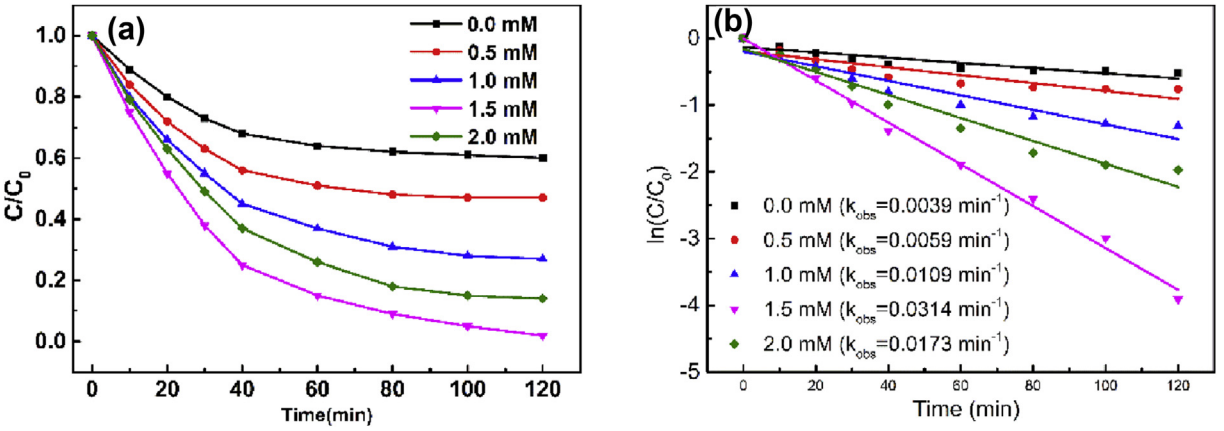

Fig. 6. (a) Effect of H_2O_2 concentration on the degradation profile of AO7 and (b) pseudo-first-order rate constant (AO 24 mg/L, PEI–AuNPs–Mn^{III}PPIX 2.4 mg/L, pH 2.0).

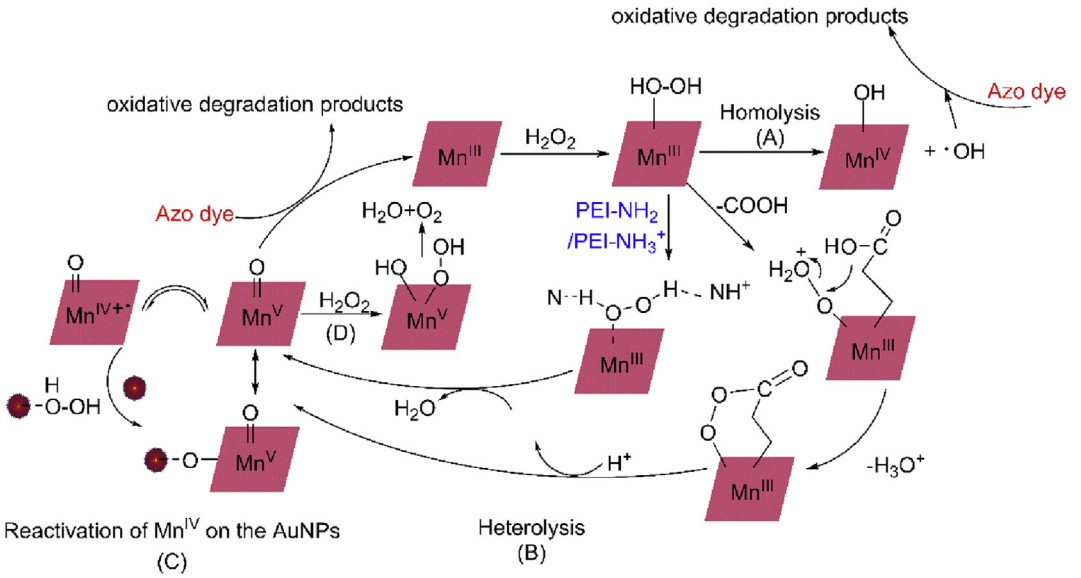

Scheme 2. Possible reaction pathways in the activation of H_2O_2 by PEI–AuNPs–Mn^{III}PPIX.

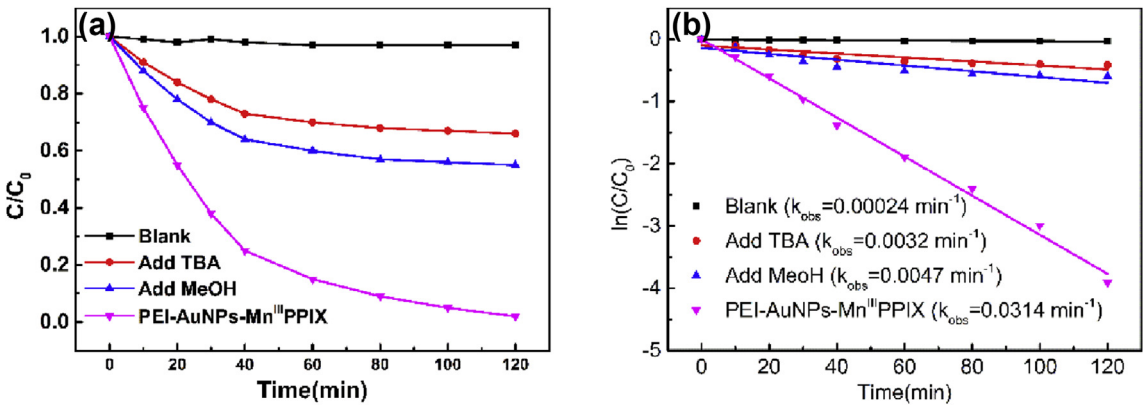

Fig. 7. (a) Effect of scavengers of •OH radicals on the degradation profile of AO7 and (b) pseudo-first-order rate constant (AO 24 mg/L, PEI–AuNPs–Mn^{III}PPIX 2.4 mg/L, pH 2.0, H_2O_2 1.5 mM).

more active high-valent metal-oxo species are produced, which are responsible for oxygen transfer to the substrate, AO7 (see Scheme 2(B)).

Second, the rich nitrogen atoms in PEI backbone, the nitrogen base, have cocatalytic effects. The similar cocatalytic effects of nitrogen bases have been reported in the catalytic reaction by Mn^{III} porphyrins [4,15,17,50]. We refer that nitrogen atoms in PET could form the hydrogen bond with H_2O_2, which may facilitate the activation of H_2O_2 as a base to promote the O–O bond cleavage, thus favoring the formation of the active catalytic species (see Scheme 2(B)). At the same time, the high density of amino groups in PEI renders the hydrophilic character of the nanocomposite. This hydrolytic stability will enhance the similarity with the natural environment of proteins and may lead to the use of practical heterogeneous catalyst in aqueous media [5].

Among the active species, Mn^{IV} species is less active and can revert to the active forms by the action of appropriate additives that induce the redox perturbation such as reduction or disproportionation [2,21,48,49], and the gold surface has been reported to have inducibility [21,49]. In PEI–AuNPs–Mn^{III}PPIX/H_2O_2 system, H_2O_2 can be activated through weak Au···O interaction with the gold surface. For Mn^{III}PPIX, the linkage between Mn–oxo to the AuNPs surface is formed and the reactivation of Mn^{IV} species to Mn^{V} species is facilitated by the linked AuNPs because of the more efficient route for electron transfer at the AuNPs surfaces (see Scheme 2(C)).

In this proposed mechanism, the excess H_2O_2 reacts with the Mn–oxo nanocomposite to produce the molecule of oxygen and water as shown in Scheme 2(D). The excess H_2O_2 also reacts with •OH radicals to produce •OOH with lower oxidation potential than that of •OH:

$$H_2O_2 + {}^{\bullet}OH \rightarrow H_2O + {}^{\bullet}OOH$$

This is why H_2O_2 concentration required is rather low in the PEI–AuNPs–Mn^{III}PPIX/H_2O_2 system, which is proved by the experiments as shown in Fig. 7.

4. Conclusion

In this work, the novel PEI–AuNPs–Mn^{III}PPIX nanocomposite with remarkable peroxidase-like activity in aqueous media was prepared under mild conditions. The nanocomposite showed high hydrolytic stability and the degradation of azo dye AO7 experiments demonstrated that the nanocomposite expresses high peroxidase-like activity in the presence of low concentration of H_2O_2. Our results in this study are one step forward in the development of a new trinary of peroxidase mimics with high activity in water. We proposed the coupling mechanism on the nature of Mn^{III}PPIX, PEI, and AuNPs involving the formation of active radicals: (1) the typical homolysis of O–O in Mn peroxide catalyzed by Mn porphyrin with generation of •OH radicals; (2) the carboxyl group in Mn^{III}PPIX affords a suitable tail for the coordination and activation of H_2O_2 due to the formation of an acyperoxy-Mn^{III} intermediate, favoring the heterolytic cleavage of the O–O bond; (3) the nitrogen atom in PEI backbone served as a base to promote the O–O bond cleavage by forming a hydrogen bond with H_2O_2; and (4) AuNPs facilitate the reactivation of Mn^{IV} species to Mn^{V} species because of the more efficient route for electron transfer at the AuNPs surfaces. The construction of the novel catalyst PEI–AuNPs–Mn^{III}PPIX offers a new insight into the application of Mn porphyrin upon activation of H_2O_2, which can induce many further reactions.

Acknowledgments

This work was supported by the National Natural Science Foundation of China (21575066).

References

[1] A. Bloodsworth, V.B. O'Donnell, I. Batinić-Haberle, P.H. Chumley, J.B. Hurt, B.J. Day, J.P. Crow, B.A. Freeman, Free Radical Biol. Med. 28 (2000) 1017.
[2] M.L. Merlau, W.J. Grande, S.B.T. Nguyen, J.T. Hupp, J. Mol. Catal. A Chem. 156 (2000) 79.
[3] A. Tovmasyan, H. Sheng, T. Weitner, A. Arulpragasam, M. Lu, D.S. Warner, Z. Vujaskovic, I. Spasojevic, I. Batinichaberle, Med. Princ. Pract. 22 (2013) 103.
[4] B. Meunier, Chem. Rev. 92 (1992) 1411.
[5] B. C Grazia, H. Madeleine, J.E. Warren, D.R. Allan, N.B. Mckeown, Science 327 (2010) 1627.
[6] S. Banfi, F. Legramandi, F. Montanari, G. Pozzi, S. Quici, J. Chem. Soc. Chem. Commun. 18 (1991) 1285.
[7] K.K. Khan, M.S. Mondal, S. Mitra, J. Chem. Soc. Dalton Trans. 6 (1996) 1059.
[8] J.-L. Primus, S. Grunenwald, P.-L. Hagedoorn, A.-M. Albrecht-Gary, D. Mandon, C. Veeger, J. Am. Chem. Soc. 124 (2002) 1214.
[9] X. Wang, Y. Lu, Biochemistry 38 (1999) 9146.
[10] M.S. Mondal, S. Mitra, Biochim. Biophys. Acta 1296 (1996) 174.
[11] A. Gengenbach, S. Syn, X. Wang, Y. Lu, Biochemistry 38 (1999) 11425.
[12] Y.B. Cai, X.H. Li, J. Jing, J.L. Zhang, Metallomics 5 (2013) 828.
[13] Y.B. Cai, S.Y. Yao, M. Hu, X. Liu, J.L. Zhang, Inorg. Chem. Front. 3 (2016) 1236.
[14] P.L. Anelli, S. Banfi, F. Legramandi, F. Montanari, G. Pozzi, S. Quici, J. Chem. Soc., Perkin Trans. 1 (1993) 1345.
[15] P. Zucca, G. Mocci, A. Rescigno, E. Sanjust, J. Mol. Catal. A Chem. 278 (2007) 220.
[16] A.C. Serra, C. Docal, A.D.A. Rocha Gonsalves, J. Mol. Catal. A Chem. 238 (2005) 192.
[17] A.L. Faria, T.O.C. Mac Leod, V.P. Barros, M.D. Assis, J. Braz. Chem. Soc. 20 (2009) 895.
[18] A. Zarrinjahan, M. Moghadam, V. Mirkhani, S. Tangestaninejad, I. Mohammadpoor-Baltork, J. Iran. Chem. Soc. 13 (2016) 1509.
[19] S. Rayati, S. Malekmohammadi, J. Exp. Nanosci. 11 (2016) 872.
[20] R. Kubota, S. Asayama, H. Kawakami, Chem. Commun. 50 (2014) 15909.
[21] Y. Murakami, K. Konishi, J.Am. Chem. Soc. 129 (2007) 14401.
[22] R.C. Pawar, S. Kang, S.H. Ahn, C.S. Lee, RSC Adv. 5 (2015) 24281.
[23] H. Tsunoyama, H. Sakurai, N. Ichikuni, Y. Negishi, T. Tsukuda, Langmuir 20 (2004) 11293.
[24] M. Ovais, A. Raza, S. Naz, N.U. Islam, A.T. Khalil, S. Ali, M.A. Khan, Z.K. Shinwari, Appl. Microbiol. Biotechnol. 101 (2017) 1.
[25] X. Fang, H. Ma, S. Xiao, M. Shen, R. Guo, X. Cao, X. Shi, J. Mater. Chem. 21 (2011) 4493.
[26] J. Han, J. Dai, L. Li, P. Fang, R. Guo, Langmuir 27 (2011) 2181.
[27] P. Veerakumar, M. Velayudham, K.-L. Lu, S. Rajagopal, Appl. Catal. A 439 (2012) 197.
[28] J. Kong, X. Yu, W. Hu, Q. Hu, S. Shui, L. Li, X. Han, H. Xie, X. Zhang, T. Wang, Analyst 140 (2015) 7792.
[29] S.V. Mohan, K.K. Prasad, N.C. Rao, P.N. Sarma, Chemosphere 58 (2005) 1097.
[30] A.P. Zhang, L. Fang, J.L. Wang, W.P. Liu, Environ. Prog. Sustain. Energy 32 (2013) 294.
[31] I. Mielgo, C. Lopez, M.T. Moreira, G. Feijoo, J.M. Lema, Biotechnol. Prog. 19 (2003) 325.
[32] P. Ollikka, T. Harjunpää, K. Palmu, P. Mäntsälä, I. Suominen, Appl. Biochem. Biotechnol. 75 (1998) 307.

[33] M. Yan, H. Xie, Q. Zhang, H. Qu, J. Shen, J. Kong, J. Mater. Sci. Chem. Eng. 4 (2016) 26.
[34] V.P. Barros, M.D. Assis, J. Braz. Chem. Soc. 24 (2013) 830.
[35] A. Córdoba, I. Magario, M.L. Ferreira, Int. Biodeterior. Biodegrad. 73 (2012) 60.
[36] S. Pirillo, F.S.G. Einschlag, E.H. Rueda, M.L. Ferreira, Ind. Eng. Chem. Res. 49 (2010) 6745.
[37] J. Chen, L. Zhao, H. Bai, G. Shi, J. Electroanal. Chem. 657 (2011) 34.
[38] C. Shan, H. Yang, D. Han, Q. Zhang, A. Ivaska, L. Niu, Biosens. Bioelectron. 25 (2010) 1070.
[39] W. Haiss, N.T.K. Thanh, J. Aveyard, D.G. Fernig, Anal. Chem. 79 (2007) 4215.
[40] F. Gholamiborujeni, A.H. Mahvi, S. Nasseri, M.A. Faramarzi, R. Nabizadeh, M. Alimohammadi, Appl. Biochem. Biotechnol 165 (2011) 1274.
[41] V. Yousefi, H.R. Kariminia, Int. Biodeterior. Biodegrad. 64 (2010) 245.
[42] Z. Wu, R. Zhang, Z. Rong, Dyest. Color. 51 (2014) 1.
[43] T.C. Bruice, M.F. Zipplies, W.A. Lee, Proc. Natl. Acad. Sci. U.S.A. 83 (1986) 4646.
[44] N.A. Zubir, C. Yacou, X. Zhang, J.C. Diniz da Costa, J. Environ. Chem. Eng. 2 (2014) 1881.
[45] J.T. Groves, J. Inorg. Biochem. 100 (2006) 434.
[46] Z. Feng, J. Yu, J. Kong, T. Wang, Chem. Eng. J. 294 (2016) 236.
[47] L. Gomathi Devi, S. Girish Kumar, K. Mohan Reddy, C. Munikrishnappa, J. Hazard Mater. 164 (2009) 459.
[48] M.L. Merlau, S.H. Cho, S.S. Sun, S.T. Nguyen, J.T. Hupp, Inorg. Chem. 44 (2005) 5523.
[49] Y. Murakami, K. Konishi, New J. Chem. 32 (2008) 2134.
[50] P. Zucca, C. Vinci, F. Sollai, A. Rescigno, E. Sanjust, J. Mol. Catal. A: Chem. 288 (2008) 97.